





# TBK1 interacts with tau and enhances neurodegeneration in tauopathy

Received for publication, December 17, 2020, and in revised form, April 29, 2021. Published, Papers in Press, May 7, 2021.  
<https://doi.org/10.1016/j.jbc.2021.100760>

Measho H. Abreha<sup>1,2,‡</sup>, Shamsideen Ojelade<sup>3,4,‡</sup>, Eric B. Dammer<sup>1,2,5</sup> , Zachary T. McEachin<sup>2,6</sup>, Duc M. Duong<sup>1,2,5</sup>, Marla Gearing<sup>2,5,7</sup>, Gary J. Bassell<sup>2,6</sup>, James J. Lah<sup>2,7</sup>, Allan I. Levey<sup>2,7</sup>, Joshua M. Shulman<sup>3,4,8,9,\*</sup>, and Nicholas T. Seyfried<sup>1,2,7,\*</sup> 

From the <sup>1</sup>Department of Biochemistry and <sup>2</sup>Center for Neurodegenerative Diseases, Emory University School of Medicine, Atlanta, Georgia, USA; <sup>3</sup>Department of Neurology, Baylor College of Medicine, Houston, Texas, USA; <sup>4</sup>Jan and Dan Duncan Neurological Research Institute, Texas Children's Hospital, Houston, Texas, USA; <sup>5</sup>Department of Pathology and Laboratory Medicine, <sup>6</sup>Department of Cell Biology, and <sup>7</sup>Department of Neurology, Emory University School of Medicine, Atlanta, Georgia, USA; <sup>8</sup>Department of Molecular and Human Genetics, Baylor College of Medicine, Houston, Texas, USA; and <sup>9</sup>Department of Neuroscience, Baylor College of Medicine, Houston, Texas, USA

Edited by Paul Fraser

One of the defining pathological features of Alzheimer's disease (AD) is the deposition of neurofibrillary tangles (NFTs) composed of hyperphosphorylated tau in the brain. Aberrant activation of kinases in AD has been suggested to enhance phosphorylation and toxicity of tau, making the responsible tau kinases attractive therapeutic targets. The full complement of tau-interacting kinases in AD brain and their activity in disease remains incompletely defined. Here, immunoaffinity enrichment coupled with mass spectrometry (MS) identified TANK-binding kinase 1 (TBK1) as a tau-interacting partner in human AD cortical brain tissues. We validated this interaction in human AD, familial frontotemporal dementia and parkinsonism linked to chromosome 17 (FTDP-17) caused by mutations in *MAPT* (R406W & P301L) and corticobasal degeneration (CBD) postmortem brain tissues as well as human cell lines. Further, we document increased TBK1 activation in both AD and FTDP-17 and map TBK1 phosphorylation sites on tau based on *in vitro* kinase assays coupled to MS. Lastly, in a *Drosophila* tauopathy model, activating expression of a conserved TBK1 ortholog triggers tau hyperphosphorylation and enhanced neurodegeneration, whereas knockdown had the reciprocal effect, suppressing tau toxicity. Collectively, our findings suggest that increased TBK1 activation may promote tau hyperphosphorylation and neuronal loss in AD and related tauopathies.

Deposition of extracellular amyloid- $\beta$  (A $\beta$ ) plaque and accumulation of intracellular neurofibrillary tangles (NFTs) composed of the microtubule-binding protein tau in the brain are the major hallmarks of Alzheimer's disease (AD) (1–3). The degree of NFT burden in the brain is closely associated with synaptic loss and cognitive decline, therefore, making tau a major therapeutic target (4, 5). Tau is a microtubule-

associated protein required for binding and stabilization of microtubules under physiological conditions (6–8). In AD, tau undergoes hyperphosphorylation among other post-translational modifications (PTMs), leading to accumulation of NFTs (1, 9). Tau phosphorylation is regulated by tau kinases and phosphatases, the aberrant levels and activity of which have been suggested to impact tau hyperphosphorylation and aggregation (10, 11). Toward this end, the identification of new tau kinases could reveal potential targets and pathways that contribute to further development of therapeutic drugs in the treatment of AD and other tauopathies.

Mass spectrometry (MS)-based proteomics has emerged as a powerful approach to define global changes in protein abundance and PTMs linked to disease mechanisms (12). MS-based proteomics can also be combined with affinity enrichment strategies, such as immunoprecipitation (IP), to identify interacting partners of key proteins linked to disease pathogenesis (13, 14). We and others have coupled co-immunoprecipitation (co-IP) with MS to identify and quantify tau-interacting partners (*i.e.*, tau interactome) in AD brain tissues (15–17). This has highlighted a diversity of tau-interacting partners having functional roles beyond a microtubule assembly, including RNA binding/splicing, translation, autophagy, and the ubiquitin-proteasome system (15–17).

To identify new tau kinases, we analyzed our previously reported tau co-IP MS datasets from control and AD brain (16). This led to the identification of 21 kinases, of which 18 have been previously described to interact or directly phosphorylate tau (18, 19). We prioritized TBK1, a serine threonine kinase belonging to the noncanonical IKK family of kinases (20, 21), best characterized for its role in innate immunity signaling (22–26), selective autophagy pathways (27–29), energy metabolism (30, 31), tumorigenesis (32), and microtubule dynamics (33). Notably, genetic studies have also identified mutations in the *TBK1* gene as causal for neurodegenerative diseases including frontotemporal dementia (FTD) and amyotrophic lateral sclerosis (ALS) (34–38). However, a role

<sup>‡</sup> These authors contributed equally to this work.

\* For correspondence: Nicholas T. Seyfried, [nseyfri@emory.edu](mailto:nseyfri@emory.edu); Joshua M. Shulman, [Joshua.Shulman@bcm.edu](mailto:Joshua.Shulman@bcm.edu).

## TBK1 phosphorylates and interacts with Tau

for TBK1 in modifying tau phosphorylation and toxicity in AD and other tauopathies is not known.

Here we report enhanced TBK1 activation and interactions with tau in AD and related tauopathies including familial frontotemporal dementia and parkinsonism linked to chromosome 17 (FTDP-17). We also identify the predominant TBK1 phosphorylation sites on tau from *in vitro* kinase assays coupled to MS. TBK1 overexpression studies in human cells and *Drosophila* neurons confirmed the role of TBK1 activation in tau hyperphosphorylation in model systems. Finally, TBK1 overexpression and knockdown in *Drosophila* can reciprocally increase and decrease tau-induced neurodegeneration. Together these data support a hypothesis that TBK1 activation may enhance tau phosphorylation and neuronal loss in AD and related tauopathies.

## Results

### Identification of novel tau-interacting kinases in AD brain

Tau kinases tightly regulate tau phosphorylation, and their aberrant activity has been previously reported in AD (11, 39). Currently, the full complement of tau-interacting kinases is not known. We previously performed tau co-IP coupled with quantitative MS analysis and identified more than 500 tau-interacting proteins in AD brain (16). Here we performed Gene Ontology (GO) analysis of the AD tau-interacting proteins, which revealed significant enrichment of terms related to kinase activity (e.g., “kinase signaling” and “kinase binding”) (Fig. 1A). Consistently, 21 of the proteins that mapped to these GO terms were kinases including several well-established tau kinases such as glycogen synthase kinase 3 $\beta$  (GSK3 $\beta$ ) (11), cyclin dependent kinase 5 (CDK5) (40), mitogen-activated protein kinases (MAPK1 and MAPK15) (19), calcium/calmodulin-dependent protein kinases (CAMK2A, CAMK2B, CAMK2D, and CAMK2G) (41), and TAOK1 (42) (Fig. 1B).

The signal intensities measured by MS for these kinases were significantly increased in AD compared with controls (Fig. 1B). To our knowledge, TNIK, DAPK3, and TBK1 (log<sub>2</sub> fold-changes 5.32, 3.96, 5.32 and  $-\log_{10} p$  values 5.99, 6.02, 1.62, respectively) have not been previously reported to interact with tau. To validate the increased interactions for two of these kinases, TBK1 and DAPK3, we performed tau co-IP from control and AD postmortem cortical brain lysates using Tau5 antibody previously used for IP-MS analysis (16). As expected, input tau levels appear stronger and showed higher- and lower-molecular-weight species observed, due to PTMs and proteolysis, respectively (43, 44) (Fig. 1C). However, the western blot for GAPDH highlights equal loading of protein across inputs. Assessment of DAPK3 and TBK1 in these inputs revealed similar levels of both DAPK3 and TBK1 in control and AD samples indicating that steady-state levels of these kinase are unchanged in disease (Fig. 1C, bottom panels). In contrast, tau co-IPs showed strong bands for both DAPK3 (~52 kDa) and TBK1 (~84 kDa) in AD suggesting increased interaction between pathological AD tau and these kinases consistent with the co-IP MS data (Fig. 1, B and D). Notably, TBK1 is a serine threonine kinase belonging to the non-canonical IKK family of kinases with roles in innate immunity signaling (20, 22) and autophagy (25, 45). We focused our attention on TBK1, as mutations in the *TBK1* gene are causal for neurodegenerative diseases including FTD and ALS (35, 37). However, a role for TBK1 in modifying tau phosphorylation and toxicity in AD and related tauopathies has not been established.

### Increased activation and tau interaction of TBK1 in AD and related tauopathies

Given that TBK1 interacts with AD tau, yet steady-state TBK1 levels remain unchanged, we hypothesized that TBK1

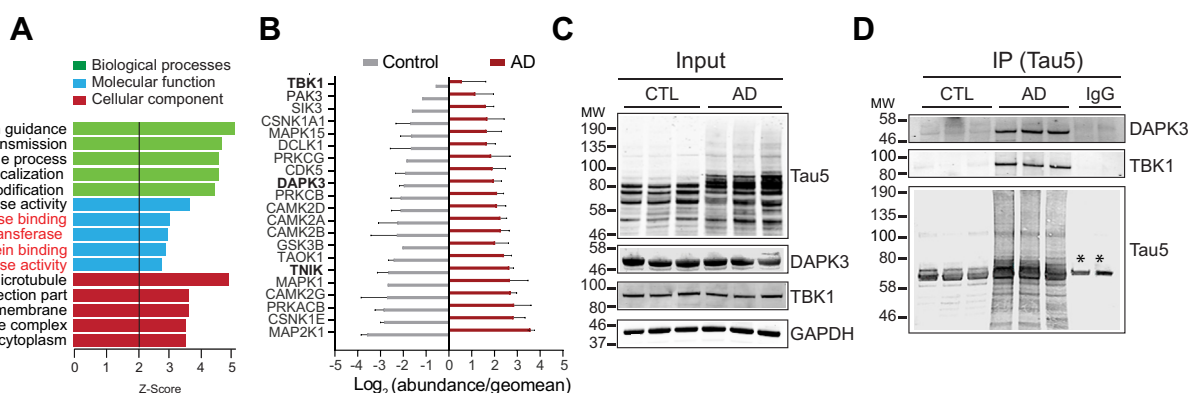


**Figure 1. IP-MS analysis of human postmortem brains identifies novel tau-interacting kinases.** A, Gene ontology (GO) analysis of AD tau-interacting proteins identified terms associated with “kinase binding,” “phosphotransferase,” “phosphoprotein binding,” and “kinase activity” (highlighted in red). B, identification and quantification of 21 tau-interacting kinases. Tau-interacting kinases were selected from our previously published tau interactome MS data generated from four control and four AD samples (16). A graph depicts increased log<sub>2</sub> intensities of tau-interacting kinases in AD (n = 4) compared with controls (n = 4) following co-IP MS as previously reported (16). The intensity for each kinase is divided by the group (AD or control) geomean and log<sub>2</sub> fold changes are plotted. All kinases had significant log<sub>2</sub>-fold increase in AD (Student’s *t*-test,  $p \leq 0.05$ ). Novel tau-interacting kinases (TBK1, DAPK3, and TNIK) are highlighted in bold. C, Western blot analysis of AD (n = 3) and control (n = 3) postmortem brain inputs using tau antibodies (Tau5) shows high-molecular-weight (HMW) tau species in AD, whereas DAPK3 (~52 kDa) and TBK1 (~84 kDa) western blots show equal levels of both kinases in AD and control samples. GAPDH was used as a loading control in inputs. D, IP of tau followed by immunoblotting for DAPK3 and TBK1 in AD brain compared with controls showed interaction of AD tau with both DAPK3 and TBK1. Lysates (pooled AD or control) incubated with isotype matched IgG were used as controls. Asterisk indicates nonspecific heavy IgG chains in negative control samples.

activation is elevated in AD brain. TBK1 activation is induced by *trans*-autophosphorylation of serine 172 (S172) in the activation loop within the kinase domain (46, 47). Therefore, to measure activated TBK1 levels, we performed western blot analysis of AD and control postmortem brain lysates with a pS172-TBK1 antibody. We observed an increase in pS172-TBK1 levels in AD brain samples (Fig. 2A), and quantification of total TBK1 and pS172-TBK1 levels shows a statistically significant (Student's *t*-test, *n* = 3, *p* value = 0.0056) increase in pS172-TBK1 in AD (Fig. 2B).

To assess whether the tau and TBK1 interaction was unique to AD or shared with other tauopathies, we first performed co-IP for tau in postmortem brain cortical tissues from an FTDP-17 case caused by a missense mutation (R406W) within the C-terminus of tau. Notably, FTDP-17 cases with this particular mutation exhibit an AD-like clinical phenotype including relatively late-onset amnesic dementia and longer disease duration as well as accumulation of hyperphosphorylated tau in NFTs (48). Like AD, the FTDP-17 (R406W) case showed increased high-molecular-weight tau species and TBK1 activation in the total brain inputs (Fig. 2C). Furthermore, tau showed increased interaction with TBK1 in FTDP-17, but not control cases following co-IP (Fig. 2D). To further assess the

specificity of this interaction across other tauopathies, we performed tau co-IPs from two additional familial cases of FTDP-17 (harboring P301L mutations) and three cases of corticobasal degeneration (CBD), a sporadic tauopathy (49). Western blot analysis of input lysates revealed high-molecular-weight tau species in the majority, but not all non-AD tauopathies compared with controls (Fig. 2, E and F), whereas the levels of TBK1 remained generally equal across all samples. Notably, TBK1 showed strong interaction with tau in AD and all non-AD tauopathies (Fig. 2F). This suggests that TBK1 has increased affinity for tau in AD and related tauopathies due to potential disease-specific phosphorylation and/or conformational changes. Thus, increased activation and interaction of TBK1 with pathologic tau may be common across these tauopathies.

**TBK1 directly phosphorylates tau**

Given that tau and TBK1 interact in AD brain, we next sought to determine whether tau was a substrate of TBK1 phosphorylation. To identify putative sites of TBK1 directed phosphorylation of tau, we performed MS analysis of TBK1 *in vitro* kinase reactions, whereby recombinant purified tau protein was incubated in kinase reaction buffer with ATP in

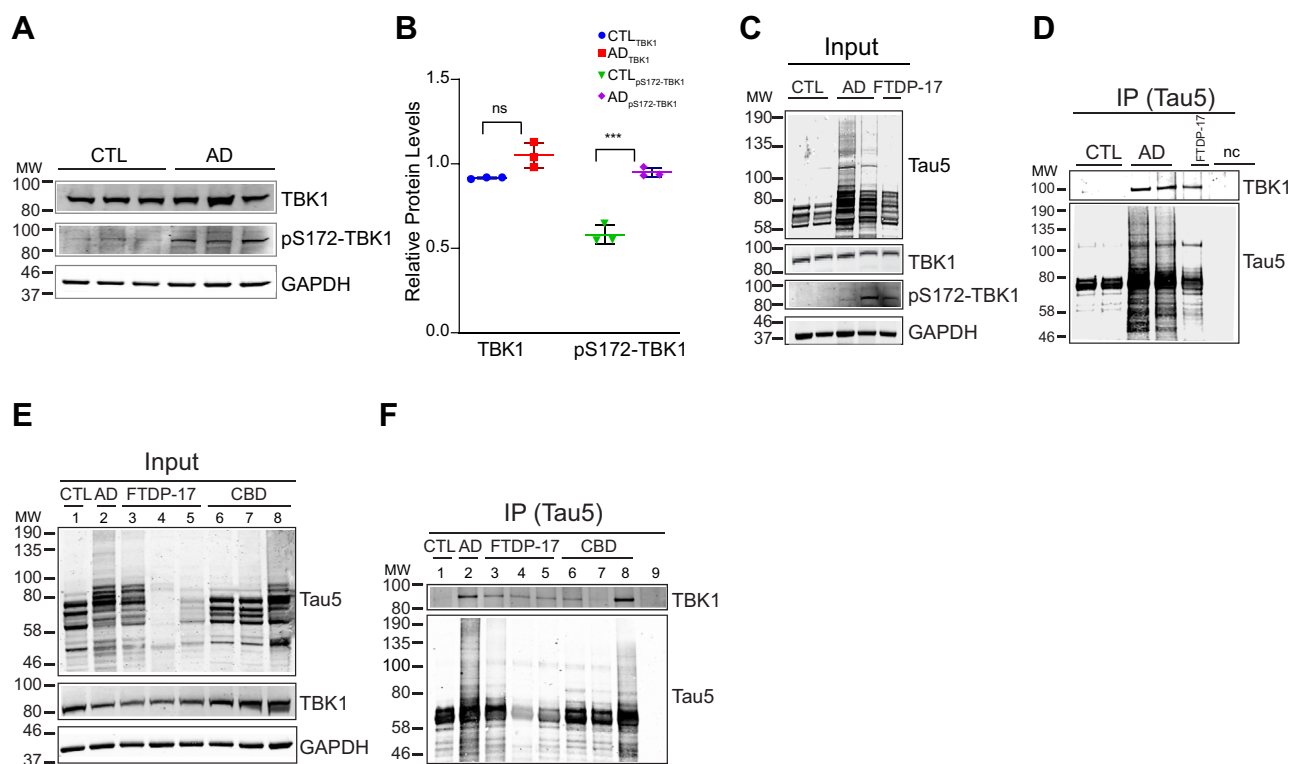


**Figure 2. Increased activation and interaction of TBK1 in AD and related tauopathies.** A, Western blot analysis of postmortem brain tissues from control and AD cases for total TBK1 and phospho-TBK1 (pS172-TBK1) in AD compared with controls. B, quantification of the pS172-TBK1 levels in AD. Each group is plotted as the mean  $\pm$  standard deviation (Student's *t*-test, *n* = 3, \*\*\* = *p* < 0.001). C, Western blot analysis of control (*n* = 2), AD (*n* = 2) and an FTDP-17 (R406W) (*n* = 1) postmortem brain inputs using total TBK1 and phospho-TBK1 (pS172-TBK1) antibodies showed increased pS172-TBK1 in AD and FTDP-17 (R406W). D, IP of tau (Tau5) followed by immunoblotting for TBK1 shows interaction of TBK1 with tau from AD (positive control) and FTDP-17 brain. Cell lysate incubated with beads alone was used as a negative control (nc). E, Western blot analysis of inputs from control (lane 1), AD (lane 2), and additional tauopathy cases: including FTDP-17 (R406W, lane 3), P301L (lanes 4 and 5), and CBD (*n* = 3) brain samples using Tau5 and TBK1 showed increased HMW tau species in AD and FTDP-17 and CBD cases (lanes 6, 7, and 8), while tau and TBK1 levels remained the same. F, Western blot analysis of tau IPs using TBK1 antibody showed interaction of tau and TBK1 in AD and other tauopathies. GAPDH was used as a loading control. Pooled (AD) lysate incubated with beads alone was used as a negative control (lane 9).

## TBK1 phosphorylates and interacts with Tau

the presence or absence of recombinant active TBK1 (pS172-TBK1). Following tryptic digestion and MS analysis of the *in vitro* reactions, we identified phosphopeptides corresponding to nine phosphorylation sites on tau (Table S1). These sites are distributed across the N-terminal acidic domain (T30), proline-rich mid-domain (S191, S198, S214), and microtubule-binding repeat (MTBR) domains (S285, S289, S305, S324, S356) of tau (Fig. 3, A and B). In support of these MS results, western blotting was performed of the *in vitro* kinase reactions using site-specific phospho-tau antibodies, which showed a gradual increase of pS214-, pS324-, and pS356-tau levels with longer incubation times (Fig. 3C). To confirm the specificity, we added increasing concentrations of a small-molecule TBK1 inhibitor, BX795 (50, 51) to the *in vitro* kinase reactions, which led to a gradual decrease in pS214-tau phosphorylation with increasing inhibitor (Fig. 3D). As expected, recombinant active TBK1 (pS172-TBK1) and total tau (Tau 5) levels remained unaltered in all conditions (Fig. 3, C and D). In summary, these *in vitro* assays confirm that tau is a direct substrate of TBK1 and that it can be blocked by a small-molecule TBK1 inhibitor.

### Increased phosphorylation of putative TBK1-directed tau phosphosites in AD brain

To assess if the *in vitro* TBK1-mediated tau phosphorylation sites are hyperphosphorylated in AD brain, we analyzed tau phosphorylation from brain phosphoproteome data generated using immobilized metal affinity chromatography (IMAC) coupled with MS (52) as well as Tau IP phosphopeptide data (15, 16). Comparison of tau phosphorylation from AD and control cortical tissues showed a significant increase in phosphorylation of tau serine/threonine residues in AD (Fig. 4A). Notably, seven out of the nine *in vitro* putative TBK1 sites were hyperphosphorylated in AD (Fig. 4A). Comparison of tau phosphorylation sites mapped in the *in vitro* TBK1 kinase

assay with tau phosphopeptides from bulk brain homogenates (52) and tau immunoprecipitates (15, 16) showed a high degree of overlap in eight out of nine putative TBK1 directed sites (S191, S198, S214, S285, S289, S305, S324, and S356), which were all elevated in AD brain (Fig. 4B and Table S2). Although these sites are not exclusively phosphorylated by TBK1, those tau sites that can be putatively modified by TBK1 are highly phosphorylated in AD, which could be potentially driven in part by the increased TBK1 activation in AD.

### TBK1 interacts with and alters tau phosphorylation in HEK-293 cell lines

To extend our *in vitro* findings, we sought to assess if TBK1 can interact with and phosphorylate tau in human cell lines. Previously, TBK1 expression in cell lines has been shown to lead to a *trans*- autophosphorylation event at S172 in TBK1 and subsequent activation (53–55). As expected, we show that TBK1 overexpression in HEK-293 cells alone is sufficient for pS172-TBK1 activation (Fig. 5A). To assess tau-TBK1 interactions in HEK-293 cells, co-IP was performed from cells overexpressing either GFP-tau alone or both GFP-tau and Myc-TBK1 (Fig. 5B). IP of recombinant tau using a GFP antibody showed strong interactions with both total TBK1 (Myc-TBK1) and phospho-TBK1 (pS172-TBK1) (Fig. 5C). Furthermore, reciprocal IPs using a Myc antibody to enrich recombinant TBK1 also showed a strong interaction between TBK1 and GFP-tau (Fig. 5D). To determine if tau domains or specific regions are sufficient and necessary for endogenous TBK1 interaction, we made several tau truncation mutants by deleting known tau domains (N-term, proline-rich domain, MTBR, and C-Term) and tau intrinsically disordered regions thought to facilitate protein–protein interactions. Notably, none of the truncation mutations was able to effectively interact with endogenous TBK1 following IP, suggesting that a

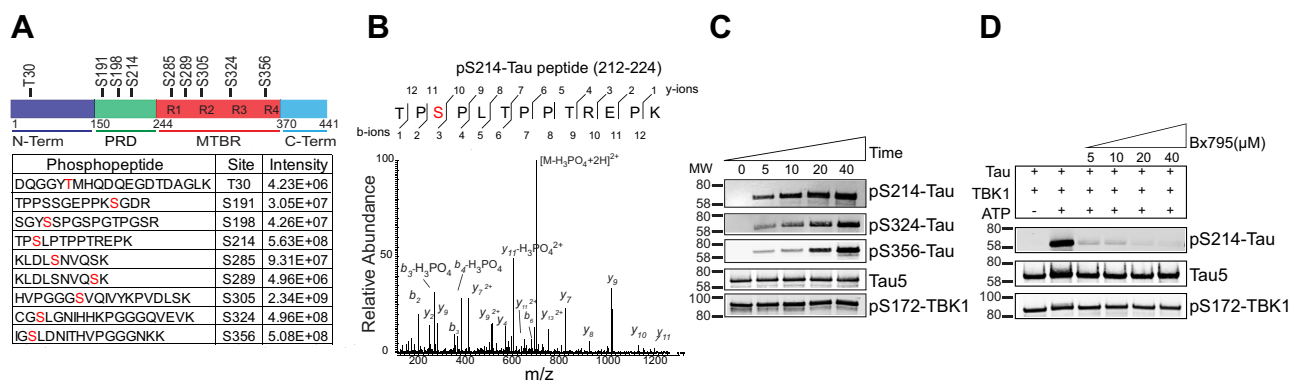


**Figure 3. TBK1 directly phosphorylates tau.** A, MS analysis of *in vitro* TBK1 kinase assay using recombinant full-length tau (1 μg) and active TBK1 (0.5 μg) was conducted in the presence of 100 μM ATP. After 30 min incubation the assay was quenched, and proteins were digested with trypsin for subsequent MS analysis. A schematic diagram depicts nine putative TBK1-mediated phosphorylation sites identified by MS across tau domains and the phosphopeptide sequences identified. N-terminus (N-term), proline-rich-domain (PRD), microtubule-binding repeats (MTBR) and C-terminus (C-term). TBK1-targeted Ser/Thr residues are indicated in red with corresponding phosphopeptide intensities measured in the mass spectrometer. B, tandem MS/MS spectrum of a tau phosphopeptide with S214 phosphorylation site (residues 212–224) shows b- and y-ions and the diagnostic neutral loss of phosphoric acid (–98 Da) on the precursor peptide. C, Western blotting of *in vitro* kinase reactions using site-specific phospho-tau antibodies (pS214, pS324, and pS356) following 0, 5, 10, 20, and 40 min (m) incubation shows gradual increase in tau phosphorylation. D, inhibition of TBK1 *in vitro* tau phosphorylation with increasing concentration (5, 10, 20, or 40 μM) of a small-molecule TBK1 inhibitor (BX795). Assays were quenched after 30 min. Western blot analysis of the *in vitro* kinase assay using pS214-Tau shows a dose-dependent decrease in S214 phosphorylation with increasing BX795 concentration. Western blots for active p172-TBK1 and total tau serve as controls.



## TBK1 phosphorylates and interacts with Tau

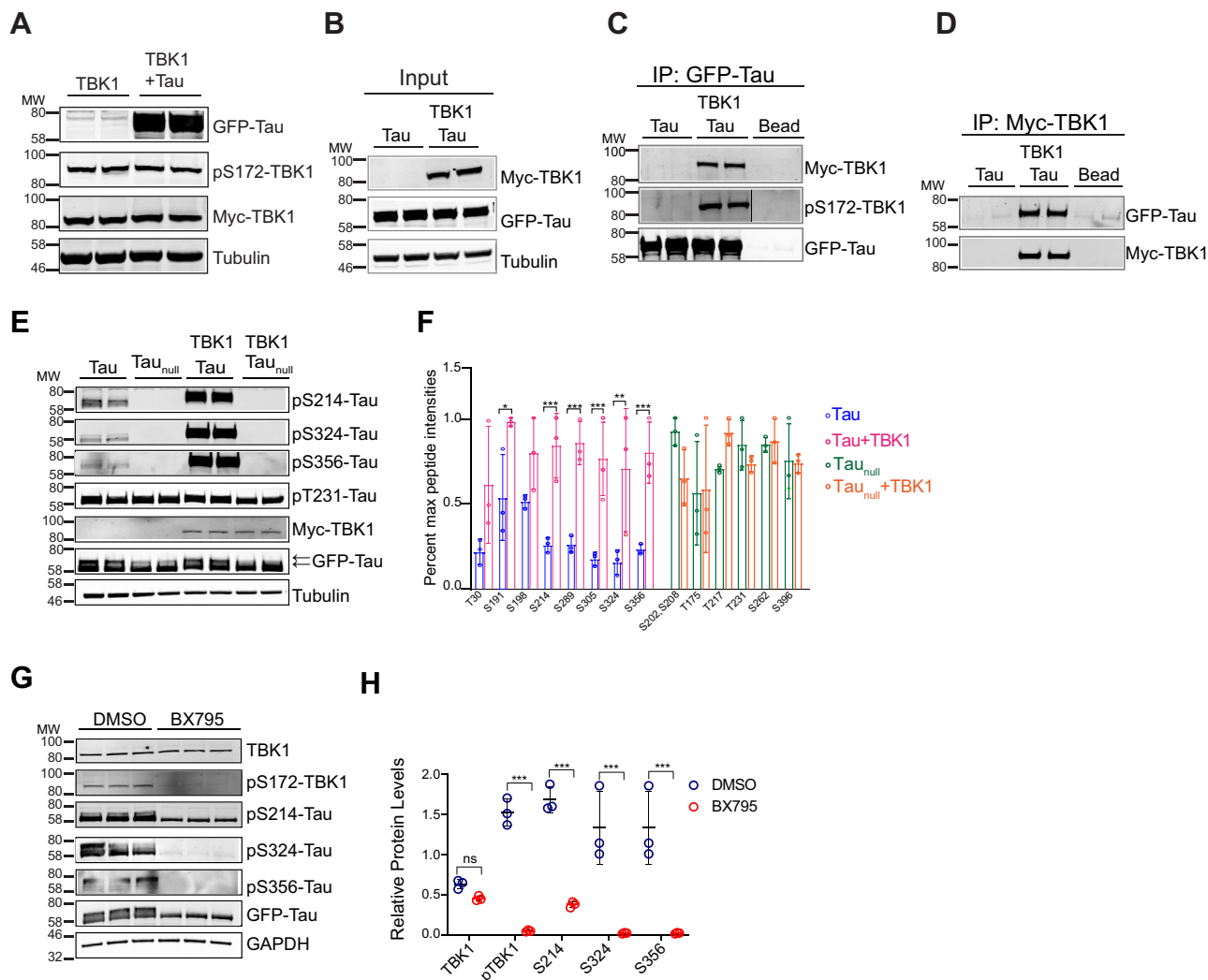


**Figure 5. TBK1 interacts with and alters tau phosphorylation in HEK-293 cell lines.** *A*, HEK-293 cells were transfected with Myc-TBK1 in the presence or absence of GFP-Tau. Western blot using pS172-TBK1 shows TBK1 activation independent of tau expression. *B*, Western blotting for Myc and GFP shows expression of both recombinant Myc-TBK1 and GFP-Tau, respectively, in cotransfected HEK-293 cell lysates (inputs). Tubulin was used as a loading control. *C*, IP of tau using a GFP antibody followed by western blotting for Myc and pS172-TBK1 antibodies shows a positive interaction of tau with total recombinant TBK1 and activated TBK1 (pS172-TBK1), respectively. Western blot for GFP served as a positive control and beads alone were used as a negative control. The bead control lane from the pS172-TBK1 blot was cropped from the same blot. *D*, IP for Myc followed by western blotting for GFP shows recombinant tau and TBK1 interaction in HEK-293 cells. Pull-downs from cells transfected with tau alone or with bead only served as negative controls. *E*, overexpression of TBK1 in HEK-293 cells results in increased tau phosphorylation. HEK-293 cells were transfected with recombinant Myc-tagged TBK1 (Myc-TBK1) and either recombinant GFP-tagged tau (GFP-Tau) or a mutant tau (GFP-Tau<sub>null</sub>) with all nine TBK1 sites substituted with alanine. Cells were harvested 48 h post-transfection and subjected to western blot analysis using phospho-tau (S214, S324, S356, and T231) and GFP antibodies. Western blot analysis shows increased tau phosphorylation at TBK1 sites (S214, S324, and S356) but not at T231. Overexpression of TBK1 results in shift in GFP-Tau phosphorylated species (upper band, arrows). In contrast, the mutant tau (Tau<sub>null</sub>) showed loss of tau phosphorylation and decreased GFP-Tau phosphorylated species (arrows). *F*, a graph shows percent max phosphopeptide intensities for *in vitro* TBK1 tau sites. Phosphopeptide enrichment using IMAC and MS analysis of HEK-293 cell lysates described above showed increased phosphorylation of tau at putative TBK1 sites following TBK1 overexpression, whereas phosphorylation at other tau sites, not TBK1 *in vitro* sites, remained unchanged. (Student's *t*-test, *n* = 3, \* ≤ 0.05, \*\* ≤ 0.01, \*\*\* ≤ 0.001). *G*, HEK-293 cells transfected with GFP-Tau were treated with 50 μM BX795 or DMSO for 6 h in triplicate. Western analysis using pS172-TBK1, phospho-Tau antibodies (S214, S324, and S356), and GFP antibodies shows decreased pS172-TBK1 and phospho-Tau signals, whereas TBK1 levels remained unchanged. *H*, quantification of protein intensities shows a significant decrease in pS172-TBK1 and phospho-tau (S214, S324, and S356) protein levels upon BX795 treatment. Protein intensities were normalized using GAPDH protein intensities (ANOVA, *n* = 3, \*\*\* = *p* < 0.001, graphs represent mean ± SD).

phosphorylated T212 and S214 are recognized by the AT100 antibody, one of the most specific correlates of tau toxicity in AD (59). Interestingly, these manipulations also revealed an overall increase in total tau protein levels following hTBK1 or dTBK1 expression. Reciprocally, knockdown of *Drosophila* TBK1, using an available transgenic *dTBK1* RNA-interference strain (60), induced relative hypophosphorylation of S214 and, overall, reduced tau protein levels in *Elav>tau<sup>R406W</sup>* animals

(Fig. 6, C–E). In order to examine if genetic manipulation of dTBK1 also modulates tau-induced neurodegeneration, we aged animals for 10 days and performed TUNEL staining to reveal neuronal death in the adult brain. *Elav>tau<sup>R406W</sup>* revealed a mild degree of TUNEL-positive nuclei, as expected. However, activating expression of dTBK1 or hTBK1 significantly increase tau-mediated neuronal death, whereas knockdown of TBK1 had the opposite effect, suppressing tau

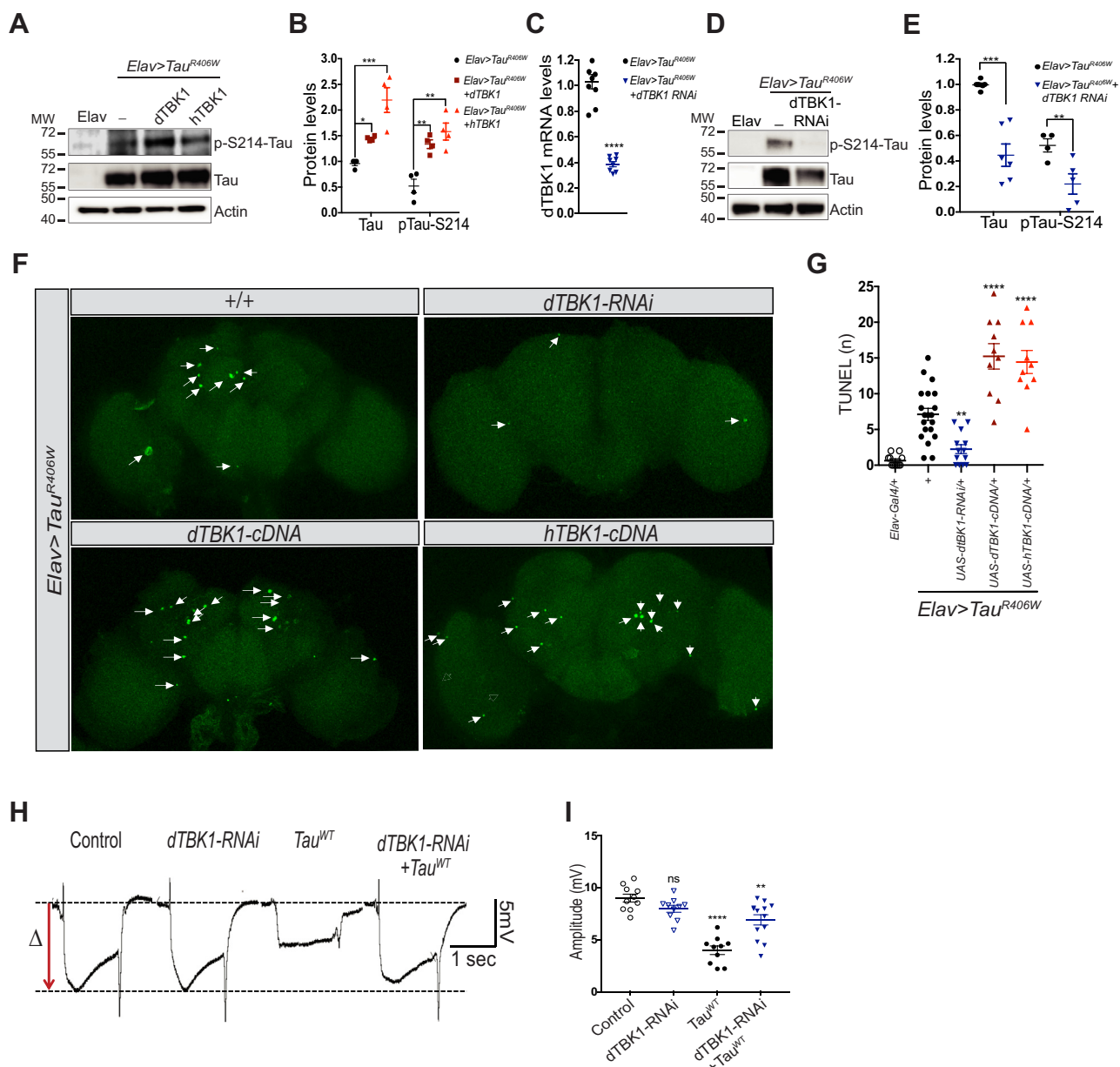


**Figure 6. Altering TBK1 expression in vivo affects tau S214 phosphorylation and neurotoxicity in flies.** A, transgenic flies expressing either *Drosophila* TBK1 (dTBK1) or human TBK1 (hTBK1) in conjunction with human mutant  $Tau^{R406W}$  in the adult brain ( $Elav>Tau^{R406W}$  + UAS hTBK1-cDNA or  $Elav>Tau^{R406W}$  + UAS dTBK1-cDNA) enhances Tau expression and S214 phosphorylation levels when compared with  $Elav>Tau^{R406W}$  and quantified in (B, n = 5). C, qPCR quantification (n = 3) shows that RNAi-mediated knockdown of dTBK1 causes a 60% loss of mRNA transcript levels in flies when compared with controls. Flies not expressing human tau (*Elav* alone) serve as negative control and show no human tau expression. D, RNAi knockdown of TBK1 suppresses tau expression and S214 phosphorylation in  $Elav>Tau^{R406W}$  flies ( $Elav>Tau^{R406W}$  + UAS dTBK1-RNAi) when compared with controls ( $Elav>Tau^{R406W}$ ) and quantified in (E, n = 5). Protein level quantification in panels B and E shows total-Tau (Tau) expression normalized to actin, and S214 phosphorylation (pTau-S214) is quantified as pS214 levels divided by normalized total-Tau. F, TUNEL staining in 10-day-old transgenic fly brains expressing either human TBK1 (hTBK1) or *Drosophila* TBK1 (dTBK1) in conjunction with human mutant  $Tau^{R406W}$  ( $Elav>Tau^{R406W}$  + UAS hTBK1-cDNA or  $Elav>Tau^{R406W}$  + UAS dTBK1-cDNA) enhances neuronal death when compared with controls ( $Elav>Tau^{R406W}$ ). In contrast, RNAi knockdown of TBK1 in  $Elav>Tau^{R406W}$  flies ( $Elav>Tau^{R406W}$  + UAS dTBK1-RNAi) suppressed neuronal death when compared with controls ( $Elav>Tau^{R406W}$ ), panels F and G). G, quantification of TUNEL-positive nuclei based on analysis of at least ten flies for each genotype. Empty symbols mean no mutant Tau expression in these animals. H, assessment of retinal function using electroretinograms (ERGs). Representative traces showing light-induced depolarization (Left) in the following genotypes: (i) Control (*Rh1-Gal4*; +/+), (ii) dTBK1-RNAi (*Rh1-Gal4*; UAS-dTBK1-RNAi/+), (iii)  $Tau^{WT}$  (*Rh1-Gal4*; UAS- $Tau^{WT}$ /+), and (iv) dTBK1-RNAi +  $Tau^{WT}$  (*Rh1-Gal4*; UAS- $Tau^{WT}$ /UAS-dTBK1-RNAi). I, RNAi knockdown of dTBK1 in transgenic flies expressing human wild-type Tau in the retina. Empty symbols mean no wild-type Tau expression in these animals. All error bars denote SEM. \* $p < 0.05$ ; \*\* $p < 0.01$ ; \*\*\* $p < 0.001$ ; \*\*\*\* $p < 0.0001$ ; ns, not significant. Statistical tests performed were Student's *t*-test (C), two-way (B, E) and one-way (G, I) ANOVA followed by Dunnett's post hoc test for multiple comparisons.

neurotoxicity (Fig. 6, F and G). Importantly, either knockdown or overexpression of TBK1 did not cause any significant neuronal death independent of tau (Fig. S3, A and B). We further confirmed genetic interactions between TBK1 and tau

using an independent, complementary assay. For these experiments,  $Tau^{WT}$  was expressed in the adult *Drosophila* retina using the *Rhodopsin1-GAL4* driver, in the presence or absence RNAi targeting dTBK1, and light-induced

## TBK1 phosphorylates and interacts with Tau

photoreceptor polarization was measured using electroretinograms (ERGs) (Fig. 6, H and I). Indeed, we found that *dTBK1* knockdown is also a suppressor of Tau<sup>WT</sup> neurotoxicity. We were unable to perform similar assessments of *TBK1* activation, since overexpression of either *dTBK1* or *hTBK1* caused ERG defects independent of tau (data not shown). Overall, our studies in *Drosophila* models show that TBK1 modulates tau-induced neurodegeneration *in vivo*, possibly via altered tau phosphorylation and levels.

### Discussion

Tau kinases play critical roles in regulating tau phosphorylation and neurofibrillary tangle formation and are considered targets for therapeutic drug development. Here, we identified TBK1 as a novel kinase that interacts with and directly phosphorylates tau. We also show increased TBK1 activation and phosphorylation of TBK1-directed sites on tau in AD and related tauopathies. TBK1 overexpression studies in human cells and *Drosophila* neurons further confirmed the role of TBK1 activation in tau hyperphosphorylation in model systems. Finally, we show that TBK1 overexpression and knockdown in *Drosophila* can reciprocally increase and decrease tau-induced neurodegeneration.

Our previous tau interactome results from human post-mortem brain tissues using co-IP and quantitative MS identified increased or “gain-of-function” interactions of several proteins in AD and found proteins related to kinase activity (16). Although several biological processes and targets were identified in this analysis, we focused our attention on kinases in this study because one key feature in the cognitive progression of AD is the appearance of aberrant phosphorylation of tau (4, 5). To this end, tau phosphorylation regulates its microtubule binding and stabilization, and in disease, tau hyperphosphorylation induces microtubule dissociation (50), which correlates with synaptic loss and neurotoxicity (6, 7, 51, 58). Thus, identifying the kinases involved in this process will advance knowledge on tau metabolism in disease. We also showed the identification of kinases such as GSK3 $\beta$ , CDK5, and CAMK2, previously shown to target tau (18, 61) highlighting the utility of our approach for mapping tau kinases. Three novel tau-interacting kinases (TNIK, DAPK3, and TBK1) were identified and TBK1 was prioritized as a candidate because of its causal role in neurodegenerative diseases including FTD and ALS (20).

Genetic studies of *TBK1* have identified nonsense, frameshift, missense, and deletion mutations in both sporadic and familial ALS, FTD, and ALS/FTD, which predominately results in the loss-of-function phenotypes that reduce levels of the kinase and pathological TDP-43 inclusions (36, 62). Loss of TBK1 function in these diseases impacts multiple protein-protein interactions and cellular pathways including autophagy and inflammation (20, 31). In contrast, TBK1 gain of function due to duplications is associated with rare genetic forms of glaucoma (63, 64). Although we did not find differences in the steady-state levels of TBK1, our findings support an increase in TBK1 activation and enhanced physical association with tau in AD and related tauopathies. Thus, TBK1

activation and mediated tau hyperphosphorylation might be a common mechanism leading to neurodegeneration observed in AD and would align with TBK1 gain of function in tauopathies. However, specific TBK1 frameshift mutations that cause FTD can present with both phosphorylated TDP-43 and tau inclusions (62) indicating a possible shared mechanism for the initiation of both TDP-43 and tau pathology *via* TBK1 activation. Given the multiple key functions of TBK1 in cells, further investigations are suggested to resolve the direct and indirect mechanisms of TBK1 activation in neurodegenerative diseases.

Our findings support the direct ability of TBK1 to modify tau-dependent neurotoxicity. Expression of human tau in the *Drosophila* brain causes neurodegeneration, and we find that activation or reduction of TBK1 homolog enhanced or suppressed tau-mediated neurotoxicity, respectively. Specifically, TBK1 manipulation affected both S214 phosphorylation state and overall levels of tau. Since S214 phosphorylation changes were robust to normalization for total levels, our *in vivo* findings are consistent with a direct impact of TBK1 on tau phosphorylation. Because tau phosphorylation is established to modulate protein synthesis, turnover, aggregation, and accumulation (65, 66), we speculate that the change in overall levels may result following tau phosphorylation. Based on prior work (67), elevated total tau levels, along with the presence of more toxic, hyperphosphorylated forms are expected to promote neuronal loss, but additional studies will be required to confirm this model.

In future investigations, it also might be interesting to manipulate TBK1 in other cell types besides neurons. Indeed, studies of mouse brain reveal TBK1 to be broadly expressed in neurons and nonneuronal cell types including microglia (68). To this end, TBK1 expression, activation, and subsequent induction of interferon signaling are increased in peripheral macrophages in response to proinflammatory stimuli such as lipopolysaccharides (LPS) and TNF- $\alpha$  (22). Similar TBK1 signaling mechanisms are proposed to occur in microglia linked to a metabolic shift from oxidative phosphorylation to glycolysis that underlies a proinflammatory phenotype (69). Moreover, TBK1 suppresses RIPK1 activation and downstream neuroinflammation associated with a loss-of-function phenotype in ALS/FTD (70). Notably, the TBK1 haploinsufficiency phenotype associated with ALS/FTD aggravates autophagy defects and early onset of motor defects, while TBK1 haploinsufficiency at later stages seems to alleviate neuroinflammation and slow disease progression in mice models (71, 72). Thus, we recognize that TBK1 likely has key roles in glia and that cell-type-specific phenotypes will likely differ upon global inhibition of TBK1 depending on the brain region and disease stage. This underscores the importance of understanding mechanistically the impact of TBK1 loss or gain of function in a cell-type-specific manner to comprehensively define substrates and signaling pathways regulated by the kinase. TBK1 has also been reported to bind to multiple adaptors depending on type of activating stimuli and subcellular localization (25, 27, 28). Therefore, TBK1 might potentially recruit other tau kinases leading to tau hyperphosphorylation.



Hence, future TBK1 interactome studies are warranted to investigate TBK1 binding to other kinases. It is also possible that TBK1 phosphorylation of tau might lead to increased adaptor protein such as 14-3-3s, which interact with tau in the brain and in turn recruit other kinases (73, 74).

Overall, the identification of TBK1 as a novel tau-modifying kinase and modifier of tau-driven neurotoxicity introduces TBK1 as a modifier of tau pathology in AD and other tauopathies. TBK1 inhibitors are actively being developed for cancer and other inflammatory autoimmune diseases (75). In this study we used BX795, a well-established TBK1 inhibitor that blocks both TBK1 and IKK $\epsilon$  (76, 77). Notably, other TBK1 inhibitors including MRT67307, derivatized from BX795, suppresses TBK1 activity with much higher specificity (76). The ability of BX795 to block TBK1-directed phosphorylation *in vitro* and in cell culture lays the foundation for future studies that investigate the impact of BX795 and additional TBK1 inhibitors on tau phosphorylation and neurotoxicity in model systems.

Ultimately, the phosphorylation of tau is a key event in the progression of AD and related tauopathies. Thus, significant research efforts have been directed at identifying the kinases involved in this process as well as developing pharmacological agents to inhibit these proteins. Here, we show that TBK1 is a *bona fide* tau kinase and that increased TBK1 activation may promote tau hyperphosphorylation and neuronal loss. These findings support future mechanistic studies that investigate the role of TBK1 as a potential therapeutic target in AD and related tauopathies.

## Experimental procedures

### Expression plasmids and antibodies

The following expression plasmids, pRK5-EGFP-tau (plasmid # 46904) and pWZL Neo Myr Flag TBK1 (plasmid # 20648), were purchased from Addgene. The TBK1 Open Reading Frame (ORF) was subcloned into pCDNA 3.1 expression plasmid (Emory Custom Cloning Core Facility). Site-directed mutagenesis was used to make the phospho-null tau ( $\tau_{\text{null}}$ ) by substituting nine alanines for serines or threonines. Tau domain and intrinsically disordered region deletion mutants were made from pRK5-EGFP-tau plasmid. Antibodies used in this study include the following: tau 5 (ThermoFisher, MA-12808), pS214-tau (Abcam, ab170892), pS324-tau (Abcam, ab109401), pS356-tau (Abcam, ab92683), GFP (Rockland, 600-101-215), pT231-Tau (Millipore, MAB50), (Cell Signaling, 2276), GAPDH (Abcam, ab8245), TBK1 (Abcam, ab40676), pS172-TBK1 (Abcam, ab109272), actin (Sigma, MAB1501), tau (Dako, A0224), and pS214-Tau (Thermo Fisher, 44-742G).

### Human postmortem brain tissues

All human postmortem brain tissues were obtained from Emory's Alzheimer's Disease Research Center (ADRC) Brain Bank with prior consent. Frontal cortex brain tissue samples from AD, FTDP-17, and control cases, matched for age, gender, and postmortem interval (PMI), were selected for the

study. Cases were selected based on Braak and CERAD scores that are neuropathologic measures of NFTs and amyloid plaque burden, respectively. Case traits are detailed in Table S4.

### Cell culture and reagents

Human embryonic kidney (HEK)-293 cells (ATCC, CRL-3216) were cultured in Dulbecco's modified Eagle's medium (Gibco, 11965-092) supplemented with 10% (v/v) fetal bovine serum (Gibco, 97068-091) and penicillin/streptomycin (Gibco, 15140-122) and maintained at 37 °C under a humidified atmosphere of 5% (v/v) CO<sub>2</sub>. For transient transfection, cells grown to 80–90% confluency were transfected with expression plasmids using JetPrime reagent (Polyplus, 114-07) according to the manufacturer's instructions. A TBK1 inhibitor BX795 (Enzo Life Sciences, ENZ-CHM189-0005) was added at the reported concentrations 24 h post transfection and further incubated for 6 h. Subsequently, cells were rinsed with cold 1× phosphate buffered saline (PBS) and harvested in NP-40 lysis buffer (25 mM Tris-HCl (pH 7.5), 150 mM NaCl, 1 mM EDTA, 1% NP-40, 5% glycerol, plus HALT protease inhibitor cocktail, (ThermoFisher, 87786)).

### Brain tissue homogenization

Human postmortem brain tissues were homogenized as previously described (16). Briefly, tissues were homogenized in lysis buffer (25 mM Tris-HCl (pH 7.5), 150 mM NaCl, 1 mM EDTA, 1% NP-40, 5% Glycerol, and HALT protease inhibitor cocktail) using a bullet blender and the protein lysate was cleared by centrifugation at 10,000g for 15 min, followed by bicinchoninic acid (BCA) analysis (Pierce, 23225) to determine protein concentration.

### Western blotting

Protein samples (25–50  $\mu$ g) were boiled in Laemmli sample buffer (BioRad, 161-0737) at 98 °C for 5 min, resolved on Bolt 4–12% Bis-Tris gels (Thermo Fisher Scientific, NW04120BOX) followed by transfer to nitrocellulose membrane using iBlot 2 dry blotting system (Thermo Fisher Scientific, IB21001). Membranes were incubated with StartingBlock buffer (Thermo Fisher, 37543) for 30 min followed by overnight incubation in primary antibodies at 4 °C. Membranes were washed with 1×Tris-buffered saline containing 0.1% Tween 20 (TBS-T) and incubated with fluorophore-conjugated secondary antibodies (AlexaFluor-680 or AlexaFluor-800) for 1 h at room temperature. Then, membranes were washed three times with TBS-T, and images were captured using an Odyssey Infrared Imaging System (LICOR Biosciences). For *Drosophila*, 10-day-old fly head lysates were isolated and prepared in Laemmli sample buffer for western blot analyses as previously described (16).

### Co-immunoprecipitation assay (co-IP)

Co-IP was done using 1 mg of protein from brain or 500  $\mu$ g HEK-293 cell lysates. Samples were first precleared by incubating with Protein A-Sepharose conjugated beads (Invitrogen, 101041) for 1 h at 4 °C. Tau 5 antibody was used for both IP-

## TBK1 phosphorylates and interacts with Tau

MS and IP-western blot analysis. Lysates were incubated with 5  $\mu\text{g}$  of primary antibodies (Tau-5, GFP, Myc) overnight at 4  $^{\circ}\text{C}$ . AD or control pooled samples incubated with beads alone or mouse IgG2a K isotype (BD pharmingen, 550339) were used as negative controls. After overnight incubation, 50  $\mu\text{l}$  of DynaBeads Protein G suspension (Invitrogen, 10003D) was incubated with lysates for 1 h. Beads were then washed three times using wash buffer (50 mM Tris-HCl, pH 8.0, 150 mM NaCl and 0.1% NP-40), rinsed once using 1 $\times$  PBS, and boiled in 40  $\mu\text{l}$  Laemmli sample loading buffer for western blot analysis as described above.

### In vitro kinase assay

*In vitro* kinase assays were performed by incubating 0.5  $\mu\text{g}$  active TBK1 (SignalChem, T02-10G-10) with 1  $\mu\text{g}$  tau (441 residues) purified recombinant proteins (SignalChem, T08-55BN-20) in kinase assay buffer (25 mM MOPS, pH 7.2, 12.5 mM  $\beta$ -glycerol-phosphate, 25 mM  $\text{MgCl}_2$ , 5 mM EGTA, 2 mM EDTA and 0.25 mM dithiothreitol (DTT)) plus 100  $\mu\text{M}$  ATP for 30 min at 37  $^{\circ}\text{C}$  (SignalChem, K01-09). TBK1 was expressed from Baculovirus expression vector in Sf9 insect cells and purified in an active form. The specific activity of TBK1 has been determined to be 290 nmol/min/mg. TBK1 kinase assay was quenched by adding 2 M urea for MS analysis. For both time course *in vitro* kinase assay and TBK1 inhibitor dose–response reactions, 400 ng of purified tau and 200 ng of active TBK1 were used and reactions were quenched by boiling at 98  $^{\circ}\text{C}$  in Laemmli sample buffer (BioRad, 161-0737) for 5 min prior to western blot analysis. For TBK1 inhibition, increasing concentrations (5, 10, 20, and 40  $\mu\text{M}$ ) of BX795 (Enzo Life Sciences, ENZ-CHM189-0005) (53, 78) were added to *in vitro* reactions. After boiling, a fraction (100 ng) of protein was used for western blot analysis.

### LC-MS/MS analysis

For MS analyses, the TBK1 *in vitro* kinase activity assay reaction was resuspended in 50  $\mu\text{l}$  of 4 M urea buffer plus 50  $\mu\text{l}$  50  $\mu\text{M}$   $\text{NH}_4\text{HCO}_3$  buffer. Proteins were reduced using 1 mM DTT for 30 min and alkylated with 5 mM iodoacetamide (IAA) for 30 min in darkness. Proteins were then digested overnight using 1  $\mu\text{g}$  trypsin (Promega) at RT. Tryptic peptides were acidified using 1% formic acid (FA) and 0.1% trifluoroacetic acid (TFA) before desalting and purification using C18 StageTips (Pierce, 87784). Peptides were eluted in 50% acetonitrile and were dried using a SpeedVac (Savant).

Dried peptides were reconstituted in peptide loading buffer (0.1% FA, 0.03% TFA, 1% acetonitrile) containing 0.2 pmol of isotopically labeled peptide calibrants (Thermo Fisher, #88321). Approximately 1  $\mu\text{g}$  of peptides was separated on homemade  $\text{C}_{18}$  fused silica column (75  $\mu\text{m}$  internal diameter) with a 140-min gradient at a rate of 400 nl/min with 3%–80% (buffer A: water with 0.1% FA and buffer B: acetonitrile with 0.1% FA). Peptides were analyzed on an Orbitrap Fusion Tribrid Mass Spectrometer (ThermoFisher). Each cycle consists of a MS1 scan (400–1500 m/z range, 50 ms maximum injection time, 120,000 resolution and an automatic gating control

target of 200,000 ion counts) collected in the orbitrap followed by higher-energy collision dissociation (HCD) MS/MS spectra (quadrupole isolation mode, 1.6 m/z isolation window, 0.5 m/z offset, 30% collision energy, 10,000 ion counts target for automatic gating control, 35 ms maximum ion time, and Orbitrap resolution of 30,000 collected in the ion trap). Dynamic exclusion was set to exclude previously sequenced precursor ions for 30 s within a 10 ppm window. Precursor ions with charge states 2–7 were included.

### MaxQuant for label-free quantitation (LFQ)

Maxquant search engine versions v1.5.5.1 and v1.6.3.4 were used to identify and quantify phosphopeptides from MS raw files for four control and four AD human postmortem brain tau IP experiments (16) and TBK1 *in vitro* kinase assay, respectively, as previously described (79) (Table S1 and Table S2).

UniProt protein sequences containing both Swiss-Prot and TrEMBL human protein sequences (90,411 target sequences downloaded April 21, 2015) were duplicated into a reverted (decoy) peptide database, searched, and used to control peptide and razor protein false discovery rate (FDR) at 1% within MaxQuant. Methionine oxidation (+15.9949 Da), asparagine and glutamine deamidation (+0.9840 Da), N-terminal acetylation (+42.0106 Da), and cysteine carbamidomethylation (+57.0215 Da) were assigned as fixed modifications while phosphorylation (+79.9663 Da) was assigned as variable modification. Tryptic peptides with only two miscleavages were included in each database search. A precursor mass tolerance of  $\pm 20$  ppm was applied prior to mass accuracy calibration and  $\pm 4.5$  ppm after internal MaxQuant calibration. Other search settings included a maximum peptide mass of 6000 Da, a minimum peptide length of six residues, 0.05 Da tolerance for high-resolution Orbitrap MS/MS scans, or 0.6 Da for low-resolution MS/MS scans obtained in the linear ion trap. The FDR for peptide spectral matches (PSMs), proteins, and site decoy fraction were all set to 1%.

### Immobilized metal affinity chromatography (IMAC) coupled to MS

HEK-293 cell lysates (1 mg) in 8M urea lysis buffer were reduced using 1 mM DTT for 30 min and alkylated with 5 mM IAA for 30 min in darkness. Samples were sequentially digested using Lys-C (Wako) and trypsin (Promega) at 30  $^{\circ}\text{C}$ . Peptides were desalted and lyophilized using HLB columns and SpeedVac, respectively. High-Select Fe-NTA phosphopeptide enrichment kit (ThermoFisher, A32992) was used for phosphopeptide enrichment following manufacturer protocol. Following enrichment LC-MS/MS was performed as previously described (80). Each sample (4  $\mu\text{l}$ ) was loaded onto a 25 cm 75  $\mu\text{m}$  ID column in-house packed with 1.7  $\mu\text{m}$  CSH beads (Waters Corporation). The gradient started at 5% buffer B (80% acetonitrile with 0.1% FA) and ended with 30% B over 80 min. This was followed by a 5-min increase to 99% B and 5-min flush at 99% B. The Fusion orbitrap mass spectrometer was operated at top speed for 3 s cycles. Each cycle consisted of

one survey scan (120,000 resolution, 400–1400 m/z range, 50 ms max injection time, and 400,000 automatic gain control) and a round of tandem MS HCD scans (1.6 m/z isolation window, 35% normalized collision energy, 15,000 resolution, 22 ms max injection time, and 50,000 automatic gain control). Only peptide ions between 2+ and 6+ charge states were chosen for MS/MS and dynamic exclusion was set for 20 s.

### **IMAC phosphopeptide analysis**

All raw files were searched using Proteome Discoverer Suite (version 2.4.1.15) against a curated Uniprot database (downloaded on August 2020 and supplemented with GFP-tau and GFP-tau<sub>null</sub> sequences for a total of 86,398 target sequences). Search parameters included the following: fully tryptic enzyme specificity, a maximum of two missed cleavages, a precursor mass tolerance of 10 ppm, and a product ion tolerance of 0.05 Da. Fixed modification for carbamidomethylation of cysteine residues (+57.02146 Da) and variable modifications for oxidation of methionine residues (+15.99492 Da); deamidation of asparagine and glutamine (+0.984 Da); and phosphorylation of serine, threonine, and tyrosine (+79.9663 Da) were considered. Percolator was used to filter PSMs and peptides to a FDR of less than 1% using target-decoy strategy. The Minora feature was used to pair peptide ion signals across runs.

### **Immunohistochemistry**

Paraffin-embedded human postmortem brain sections (frontal cortex, 5  $\mu$ m) were deparaffinized in Histo-clear (National Diagnostics) and rehydrated in ethanol. Antigen retrieval was performed in ddH<sub>2</sub>O by steam heat for 30 min. Endogenous peroxidase activity was quenched using hydrogen peroxide and washed 3 $\times$  in TBS-T. Tissues were blocked with serum-free protein block (Dako) for 1 h. Primary antibodies were diluted in antibody diluent (Dako) and applied for 45 min at room temp. Tissue sections were subsequently washed 3 $\times$  in TBS-T and horseradish-peroxidase- (HRP)-conjugated secondaries (Dako) were applied for 30 min at room temperature. 3,3'-diaminobenzidine (DAB) was used for visualization of peroxidase labeling. Sections were counterstained with Gill's hematoxylin and blued in Scott's tap water substitute. Images were acquired using Olympus BX51 20 $\times$  and 60 $\times$  objectives.

### **Gene Ontology (GO) enrichment and hierarchical clustering analysis**

Functional enrichment of differentially expressed proteins was determined using the GO-Elite (v1.2.5) python package as previously described (81, 82). Briefly, GO-Elite Hs (human) databases were downloaded on or after June 2016. The set of all proteins identified in the tau co-IP proteomic analyses was used as the background (16). Z score and one-tailed Fisher's exact test (Benjamini–Hochberg FDR corrected) were used to assess the significance of the Z score. A cutoff of 1.96 (*p* value cutoff of 0.01 and a minimum of five genes per ontology) was used as filter prior to pruning the ontologies. Clustering analysis on differentially abundant phospho-modified peptides was performed as described before (81) with the R NMF

package in Microsoft R open v3.3. Age, sex, and PMI-regressed log<sub>2</sub> abundances were converted to Z scores (mean centered abundance, fold of standard deviation) and clustered with Euclidian distance metric, complete method of the hclust function called from NMF package aheatmap function.

### **Drosophila genetics**

Flies were raised on molasses-based food grown at 20 °C until eclosion and then placed at 25 °C for 10 days. Fly strains were obtained from the Bloomington *Drosophila* Stock Center and from the FlyORE. The *Drosophila* ortholog of Human TBK1 is *IKK-epsilon* (IKK $\epsilon$  or ik2) and is referred to in this article as dTBK1. The full genotypes of the UAS-transgenic fly lines used for manipulations of TBK1 activity are as follows: UAS-*dTBK1*-RNAi(P{TRIP.GL00160}attP2, BDSC\_35266; Flybase ID: FBal0262637), UAS-*dTBK1*-cDNA (M{UAS-IKK $\epsilon$ .ORF.3xHA}ZH-86Fb, FlyORF\_F001016; Flybase ID: FBst0500628), and UAS-*hTBK1*-cDNA (PBac{UAS-hTBK1.HA}, FlyORF\_77971; Flybase ID: FBst0077971). *Elav<sup>c155</sup>-Gal4* flies were used to drive expression of UAS lines pan-neuronally in the adult fly brain and the transgenic tauopathy model used in this article expresses human mutant Tau (UAS-Tau<sup>R406W</sup>) and human wild-type Tau (UAS-Tau<sup>WT</sup>) (57).

### **Quantitative real-time PCR (qRT-PCR)**

Total RNA was extracted from approximately 100 adult fly heads (for each genotype), equally divided between males and females. Frozen fly heads were homogenized in Trizol (Invitrogen, 15596026), treated with DNaseI (Promega, M6101), and total RNA was extracted using the RNeasy Micro Kit (QIAGEN, 74004). Following reverse transcription using the SuperScript III First-Strand Synthesis System (Invitrogen), qRT-PCR was performed using iQ SYBR Green Supermix (Bio-Rad) in a CFX96 Touch Real-Time PCR Detection System (Bio-Rad) with standard cycling parameters. Each reaction was performed in triplicate. RpL32 was used as a control for normalization of each sample to calculate delta cycle threshold (DcT) values.

### **Drosophila terminal deoxynucleotidyl transferase dUTP nick end labeling (TUNEL) assay**

TUNEL staining was performed using the FragEL DNA Fragmentation Detection Kit from Calbiochem (EMD Millipore). Ten-day-old adult fly brains were dissected in PBS-T and then fixed in 4% paraformaldehyde for 20 min on ice. Brains were washed with 1 $\times$  phosphate-buffered saline with 0.1% Tween 20 (PBS-T) 4 times for 15 min and then blocked overnight with 5% normal goat serum (NGS) in PBS-T at 4 °C. Brains were then incubated in 100 mM Sodium Citrate with 10% Triton x-100 for 30 min at 65 °C and then washed three times with PBST at room temperature. Brains were equilibrated for 15 min at room temperature and then incubated in a 1:9 mixture of terminal deoxynucleotidyl transferase (Tdt) enzyme and Tdt Labeling Buffer for 2–3 h at 37 °C. Brains were washed four times for 15 min at room temperature and then mounted on slides with Vectashield (with DAPI). Images were acquired

## TBK1 phosphorylates and interacts with Tau

using Z stack with a 2.00 step at 20× using a SP8 Leica confocal microscope and apoptotic neurons were counted.

### *Drosophila* electroretinograms (ERG)

ERG recordings were performed as previously described (83). In brief, 10-day-old adult flies were anesthetized and glued to a glass slide, with electrodes placed on the corneal surface and the thorax. Flies were maintained in the dark for at least 1 min prior to stimulation using a train of alternating light/dark pulses. Retinal responses were recorded and analyzed using LabChart software (ADInstruments). At least eight flies were examined for each genotype.

### Data availability

The mass spectrometry proteomics data from the Tau co-IPs from human postmortem brain, *in vitro* TBK1-Tau kinase assays, and HEK IMAC have been deposited to <https://www.synapse.org/> with synapse IDs, syn22150694, syn22150851, and syn25551492, respectively.

**Supporting information**—This article contains supporting information (16).

**Acknowledgments**—We would like to thank members of the Seyfried lab including Dr Sruti Rayaprolu, Sean Kundinger, and Dr Priitha Bagchi for their feedback. Support for this research was provided by funding from the National Institute on Aging (R01AG050631, R01AG053960, R01AG061800, RF1AG057471, RF1AG057470, R01AG057339), the Accelerating Medicine Partnership (AMP) for AD (U01AG061357) and the Emory Alzheimer's Disease Research Center (P50AG025688).

**Author contributions**—M. H. A. and N. T. S. conceptualization; M. H. A., S. O., E. B. D., Z. T. M., D. M. D., J. M. S., and N. T. S. methodology; M. H. A., S. O., D. M. D., and E. B. D. investigation; M. H. A., S. O., E. B. D., J. M. S., and N. T. S. formal analysis; M. H. A., S. O., J. M. S., and N. T. S. writing—original draft; M. H. A., S. O., E. B. D., D. M. D., M. G., G. J. B., J. J. L., A. I. L., J. M. S., and N. T. S. writing—review and editing; A. I. L., J. M. S., S. O., and N. T. S. funding acquisition; M. G., A. I. L., J. M. S., M. G., G. J. B., and N. T. S. resources; and J. M. S. and N. T. S. supervision.

**Funding and additional information**—S. O. was supported by a Postdoctoral Enrichment Program Award from the Burroughs Wellcome Fund (BWF-1017399) and an Alzheimer's Association fellowship (AARFD-16-442630).

**Conflict of interest statement**—The authors declare that they have no conflicts of interest with the contents of this article.

**Abbreviations**—The abbreviations used are: A $\beta$ , amyloid- $\beta$ ; AD, Alzheimer's disease; ALS, amyotrophic lateral sclerosis; CAMK, calcium/calmodulin-dependent protein kinase; CBD, corticobasal degeneration; CDK5, cyclin dependent kinase 5; co-IP, co-immunoprecipitation; DTT, dithiothreitol; ERG, electroretinogram; FA, formic acid; FDR, false discovery rate; FTD, frontotemporal dementia; FTDP-17, familial frontotemporal dementia and parkinsonism linked to chromosome 17; GO, gene ontology; GSK3 $\beta$ , glycogen synthase kinase 3 $\beta$ ; HCD, higher-energy collision

dissociation; IAA, iodoacetamide; IMAC, immobilized metal affinity chromatography; IP, immunoprecipitation; LFQ, label-free quantitation; MAPK, mitogen-activated protein kinase; MS, mass spectrometry; NFT, neurofibrillary tangle; PTM, posttranslational modification; TBK1, TANK-binding kinase 1; TFA, trifluoroacetic acid.

### References

1. Alonso, A. d. C., Grundke-Iqbal, I., and Iqbal, K. (1996) Alzheimer's disease hyperphosphorylated tau sequesters normal tau into tangles of filaments and disassembles microtubules. *Nat. Med.* **2**, 783–787
2. Bancher, C., Brunner, C., Lassmann, H., Budka, H., Jellinger, K., Wiche, G., Seitelberger, F., Grundke-Iqbal, I., Iqbal, K., and Wisniewski, H. (1989) Accumulation of abnormally phosphorylated  $\tau$  precedes the formation of neurofibrillary tangles in Alzheimer's disease. *Brain Res.* **477**, 90–99
3. Goedert, M., Spillantini, M., Jakes, R., Rutherford, D., and Crowther, R. (1989) Multiple isoforms of human microtubule-associated protein tau: Sequences and localization in neurofibrillary tangles of Alzheimer's disease. *Neuron* **3**, 519–526
4. Arriagada, P. V., Growdon, J. H., Hedley-Whyte, E. T., and Hyman, B. T. (1992) Neurofibrillary tangles but not senile plaques parallel duration and severity of Alzheimer's disease. *Neurology* **42**, 631–639
5. Bierer, L. M., Hof, P. R., Purohit, D. P., Carlin, L., Schmeidler, J., Davis, K. L., and Perl, D. P. (1995) Neocortical neurofibrillary tangles correlate with dementia severity in Alzheimer's disease. *Arch. Neurol.* **52**, 81–88
6. Alonso, A. C., Grundke-Iqbal, I., and Iqbal, K. (1996) Alzheimer's disease hyperphosphorylated tau sequesters normal tau into tangles of filaments and disassembles microtubules. *Nat. Med.* **2**, 783–787
7. Alonso, A. C., Zaidi, T., Grundke-Iqbal, I., and Iqbal, K. (1994) Role of abnormally phosphorylated tau in the breakdown of microtubules in Alzheimer disease. *Proc. Natl. Acad. Sci. U. S. A.* **91**, 5562–5566
8. Kopke, E., Tung, Y. C., Shaikh, S., Alonso, A. C., Iqbal, K., and Grundke-Iqbal, I. (1993) Microtubule-associated protein tau. Abnormal phosphorylation of a non-paired helical filament pool in Alzheimer disease. *J. Biol. Chem.* **268**, 24374–24384
9. Wesseling, H., Mair, W., Kumar, M., Schaffner, C. N., Tang, S., Beer-eppot, P., Fatou, B., Guise, A. J., Cheng, L., Takeda, S., Muntel, J., Rotunno, M. S., Dujardin, S., Davies, P., Kosik, K. S., et al. (2020) Tau PTM profiles identify patient heterogeneity and stages of Alzheimer's disease. *Cell* **183**, 1699–1713.e13
10. Gong, C. X., Shaikh, S., Wang, J. Z., Zaidi, T., Grundke-Iqbal, I., and Iqbal, K. (1995) Phosphatase activity toward abnormally phosphorylated  $\tau$ : Decrease in Alzheimer disease brain. *J. Neurochem.* **65**, 732–738
11. Liu, S. J., Zhang, A. H., Li, H. L., Wang, Q., Deng, H. M., Netzer, W. J., Xu, H., and Wang, J. Z. (2003) Overactivation of glycogen synthase kinase-3 by inhibition of phosphoinositol-3 kinase and protein kinase C leads to hyperphosphorylation of tau and impairment of spatial memory. *J. Neurochem.* **87**, 1333–1344
12. Ong, S.-E., and Mann, M. (2005) Mass spectrometry-based proteomics turns quantitative. *Nat. Chem. Biol.* **1**, 252–262
13. Ewing, R. M., Chu, P., Elisma, F., Li, H., Taylor, P., Climie, S., McBroom-Cerajewski, L., Robinson, M. D., O'Connor, L., and Li, M. (2007) Large-scale mapping of human protein–protein interactions by mass spectrometry. *Mol. Syst. Biol.* **3**
14. Gingras, A.-C., Gstaiger, M., Raught, B., and Aebersold, R. (2007) Analysis of protein complexes using mass spectrometry. *Nat. Rev. Mol. Cell Biol.* **8**, 645
15. Drummond, E., Pires, G., MacMurray, C., Askenazi, M., Nayak, S., Bourdon, M., Safar, J., Ueberheide, B., and Wisniewski, T. (2020) Phosphorylated tau interactome in the human Alzheimer's disease brain. *Brain* **143**, 2803–2817
16. Hsieh, Y. C., Guo, C., Yalamanchili, H. K., Abreha, M., Al-Ouran, R., Li, Y., Dammer, E. B., Lah, J. J., Levey, A. I., Bennett, D. A., De Jager, P. L., Seyfried, N. T., Liu, Z., and Shulman, J. M. (2019) Tau-mediated

- disruption of the spliceosome triggers cryptic RNA splicing and neurodegeneration in Alzheimer's disease. *Cell Rep.* **29**, 301–316.e310
17. Meier, S., Bell, M., Lyons, D. N., Ingram, A., Chen, J., Gensel, J. C., Zhu, H., Nelson, P. T., and Abisambra, J. F. (2015) Identification of novel tau interactions with endoplasmic reticulum proteins in Alzheimer's disease brain. *J. Alzheimers Dis.* **48**, 687–702
  18. Martin, L., Latypova, X., Wilson, C. M., Magnaudeix, A., Perrin, M. L., Yardin, C., and Terro, F. (2013) Tau protein kinases: Involvement in Alzheimer's disease. *Ageing Res. Rev.* **12**, 289–309
  19. Cavallini, A., Brewerton, S., Bell, A., Sargent, S., Glover, S., Hardy, C., Moore, R., Calley, J., Ramachandran, D., and Poidinger, M. (2013) An unbiased approach to identifying tau kinases that phosphorylate tau at sites associated with Alzheimer disease. *J. Biol. Chem.* **288**, 23331–23347
  20. Ahmad, L., Zhang, S. Y., Casanova, J. L., and Sancho-Shimizu, V. (2016) Human TBK1: A gatekeeper of neuroinflammation. *Trends Mol. Med.* **22**, 511–527
  21. Oakes, J. A., Davies, M. C., and Collins, M. O. (2017) TBK1: A new player in ALS linking autophagy and neuroinflammation. *Mol. Brain* **10**, 5
  22. Fitzgerald, K. A., McWhirter, S. M., Faia, K. L., Rowe, D. C., Latz, E., Golenbock, D. T., Coyle, A. J., Liao, S.-M., and Maniatis, T. (2003) IKK $\epsilon$  and TBK1 are essential components of the IRF3 signaling pathway. *Nat. Immunol.* **4**, 491
  23. Hemmi, H., Takeuchi, O., Sato, S., Yamamoto, M., Kaisho, T., Sanjo, H., Kawai, T., Hoshino, K., Takeda, K., and Akira, S. (2004) The roles of two I $\kappa$ B kinase-related kinases in lipopolysaccharide and double stranded RNA signaling and viral infection. *J. Exp. Med.* **199**, 1641–1650
  24. Tanaka, Y., and Chen, Z. J. (2012) STING specifies IRF3 phosphorylation by TBK1 in the cytosolic DNA signaling pathway. *Sci. signaling* **5**, ra20
  25. Weidberg, H., and Elazar, Z. (2011) TBK1 mediates crosstalk between the innate immune response and autophagy. *Sci. signaling* **4**, pe39
  26. Yu, T., Yi, Y. S., Yang, Y., Oh, J., Jeong, D., and Cho, J. Y. (2012) The pivotal role of TBK1 in inflammatory responses mediated by macrophages. *Mediators Inflamm.* **2012**, 979105
  27. He, L., Chen, L., and Li, L. (2017) The TBK1-OPTN Axis mediates crosstalk between mitophagy and the innate immune response: A potential therapeutic target for neurodegenerative diseases. *Neurosci. Bull.* **33**, 354–356
  28. Heo, J.-M., Ordureau, A., Paulo, J. A., Rinehart, J., and Harper, J. W. (2015) The PINK1-PARKIN mitochondrial ubiquitylation pathway drives a program of OPTN/NDP52 recruitment and TBK1 activation to promote mitophagy. *Mol. Cell.* **60**, 7–20
  29. Matsumoto, G., Shimogori, T., Hattori, N., and Nukina, N. (2015) TBK1 controls autophagosomal engulfment of polyubiquitinated mitochondria through p62/SQSTM1 phosphorylation. *Hum. Mol. Genet.* **24**, 4429–4442
  30. Reilly, S. M., Chiang, S.-H., Decker, S. J., Chang, L., Uhm, M., Larsen, M. J., Rubin, J. R., Mowers, J., White, N. M., and Hochberg, I. (2013) An inhibitor of the protein kinases TBK1 and IKK- $\epsilon$  improves obesity-related metabolic dysfunctions in mice. *Nat. Med.* **19**, 313
  31. Zhao, P., Wong, K. L., Sun, X., Reilly, S. M., Uhm, M., Liao, Z., Skorobogatko, Y., and Sautel, A. R. (2018) TBK1 at the crossroads of inflammation and energy homeostasis in adipose tissue. *Cell* **172**, 731–743.e712
  32. Ou, Y. H., Torres, M., Ram, R., Formstecher, E., Roland, C., Cheng, T., Brekken, R., Wurz, R., Tasker, A., Polverino, T., Tan, S. L., and White, M. A. (2011) TBK1 directly engages Akt/PKB survival signaling to support oncogenic transformation. *Mol. Cell* **41**, 458–470
  33. Pillai, S., Nguyen, J., Johnson, J., Haura, E., Coppola, D., and Chellappan, S. (2015) Tank binding kinase 1 is a centrosome-associated kinase necessary for microtubule dynamics and mitosis. *Nat. Commun.* **6**, 1–14
  34. Borghero, G., Pugliatti, M., Marrosu, F., Marrosu, M. G., Murru, M. R., Floris, G., Cannas, A., Occhineri, P., Cau, T. B., Loi, D., Ticca, A., Traccis, S., Manera, U., Canosa, A., Moglia, C., et al. (2016) TBK1 is associated with ALS and ALS-FTD in Sardinian patients. *Neurobiol. Aging* **43**, 180.e1–180.e5
  35. Freischmidt, A., Müller, K., Ludolph, A. C., Weishaupt, J. H., and Andersen, P. M. (2017) Association of mutations in TBK1 with sporadic and familial amyotrophic lateral sclerosis and frontotemporal dementia. *JAMA Neurol.* **74**, 110–113
  36. Freischmidt, A., Wieland, T., Richter, B., Ruf, W., Schaeffer, V., Müller, K., Marroquin, N., Nordin, F., Hübers, A., and Weydt, P. (2015) Haploinsufficiency of TBK1 causes familial ALS and fronto-temporal dementia. *Nat. Neurosci.* **18**, 631
  37. Gijssels, I., Van Mossevelde, S., van der Zee, J., Sieben, A., Philtjens, S., Heeman, B., Engelborghs, S., Vandenbulcke, M., De Baets, G., and Bäumer, V. (2015) Loss of TBK1 is a frequent cause of frontotemporal dementia in a Belgian cohort. *Neurology* **85**, 2116–2125
  38. Williams, K. L., McCann, E. P., Fifita, J. A., Zhang, K., Duncan, E. L., Leo, P. J., Marshall, M., Rowe, D. B., Nicholson, G. A., and Blair, I. P. (2015) Novel TBK1 truncating mutation in a familial amyotrophic lateral sclerosis patient of Chinese origin. *Neurobiol. Aging* **36**, 3334.e1–3334.e5
  39. Cruz, J. C., Tseng, H.-C., Goldman, J. A., Shih, H., and Tsai, L.-H. (2003) Aberrant Cdk5 activation by p25 triggers pathological events leading to neurodegeneration and neurofibrillary tangles. *Neuron* **40**, 471–483
  40. Paudel, H. K., Lew, J., Ali, Z., and Wang, J. (1993) Brain proline-directed protein kinase phosphorylates tau on sites that are abnormally phosphorylated in tau associated with Alzheimer's paired helical filaments. *J. Biol. Chem.* **268**, 23512–23518
  41. Litersky, J. M., Johnson, G. V., Jakes, R., Goedert, M., Michael, L., and Seubert, P. (1996) Tau protein is phosphorylated by cyclic AMP-dependent protein kinase and calcium/calmodulin-dependent protein kinase II within its microtubule-binding domains at Ser-262 and Ser-356. *Biochem. J.* **316**, 655–660
  42. Giacomini, C., Koo, C. Y., Yankova, N., Tavares, I. A., Wray, S., Noble, W., Hanger, D. P., and Morris, J. D. H. (2018) A new TAO kinase inhibitor reduces tau phosphorylation at sites associated with neurodegeneration in human tauopathies. *Acta Neuropathol. Commun.* **6**, 37
  43. Alonso, A., Zaidi, T., Novak, M., Grundke-Iqbal, I., and Iqbal, K. (2001) Hyperphosphorylation induces self-assembly of tau into tangles of paired helical filaments/straight filaments. *Proc. Natl. Acad. Sci. U. S. A.* **98**, 6923–6928
  44. Takeda, S., Wegmann, S., Cho, H., DeVos, S. L., Commins, C., Roe, A. D., Nicholls, S. B., Carlson, G. A., Pitstick, R., Nobuhara, C. K., Costantino, I., Frosch, M. P., Muller, D. J., Irimia, D., and Hyman, B. T. (2015) Neuronal uptake and propagation of a rare phosphorylated high-molecular-weight tau derived from Alzheimer's disease brain. *Nat. Commun.* **6**, 8490
  45. Pilli, M., Arko-Mensah, J., Ponpuak, M., Roberts, E., Master, S., Mandell, M. A., Dupont, N., Ornatowski, W., Jiang, S., and Bradfute, S. B. (2012) TBK-1 promotes autophagy-mediated antimicrobial defense by controlling autophagosome maturation. *Immunity* **37**, 223–234
  46. Larabi, A., Devos, J. M., Ng, S. L., Nanao, M. H., Round, A., Maniatis, T., and Panne, D. (2013) Crystal structure and mechanism of activation of TANK-binding kinase 1. *Cell Rep.* **3**, 734–746
  47. Ma, X., Helgason, E., Phung, Q. T., Quan, C. L., Iyer, R. S., Lee, M. W., Bowman, K. K., Starovasnik, M. A., and Dueber, E. C. (2012) Molecular basis of Tank-binding kinase 1 activation by transautophosphorylation. *Proc. Natl. Acad. Sci. U. S. A.* **109**, 9378–9383
  48. Lindquist, S. G., Holm, I. E., Schwartz, M., Law, I., Stokholm, J., Batbayli, M., Waldemar, G., and Nielsen, J. E. (2008) Alzheimer disease-like clinical phenotype in a family with FTDP-17 caused by a MAPT R406W mutation. *Eur. J. Neurol.* **15**, 377–385
  49. Kouri, N., Carlomagno, Y., Baker, M., Liesinger, A. M., Caselli, R. J., Wszolek, Z. K., Petrucelli, L., Boeve, B. F., Parisi, J. E., and Josephs, K. A. (2014) Novel mutation in MAPT exon 13 (p. N410H) causes corticobasal degeneration. *Acta Neuropathol.* **127**, 271–282
  50. Lindwall, G., and Cole, R. D. (1984) Phosphorylation affects the ability of tau protein to promote microtubule assembly. *J. Biol. Chem.* **259**, 5301–5305
  51. Brandt, R., Lee, G., Teplow, D. B., Shalloway, D., and Abdel-Ghany, M. (1994) Differential effect of phosphorylation and substrate modulation on tau's ability to promote microtubule growth and nucleation. *J. Biol. Chem.* **269**, 11776–11782
  52. Ping, L., Kunding, S. R., Duong, D. M., Yin, L., Gearing, M., Lah, J. J., Levey, A. I., and Seyfried, N. T. (2020) Global quantitative analysis of the human brain proteome and phosphoproteome in Alzheimer's disease. *Sci. Data* **7**, 1–13

## TBK1 phosphorylates and interacts with Tau

53. Clark, K., Plater, L., Pegg, M., and Cohen, P. (2009) Use of the pharmacological inhibitor BX795 to study the regulation and physiological roles of TBK1 and I $\kappa$ B Kinase - a distinct upstream kinase mediates Ser-172 phosphorylation and activation. *J. Biol. Chem.* **284**, 14136–14146
54. Helgason, E., Phung, Q. T., and Dueber, E. C. (2013) Recent insights into the complexity of tank-binding kinase 1 signaling networks: The emerging role of cellular localization in the activation and substrate specificity of TBK1. *FEBS Lett.* **587**, 1230–1237
55. Ma, X., Helgason, E., Phung, Q. T., Quan, C. L., Iyer, R. S., Lee, M. W., Bowman, K. K., Starovasnik, M. A., and Dueber, E. C. (2012) Molecular basis of Tank-binding kinase 1 activation by transautophosphorylation. *Proc. Natl. Acad. Sci.* **109**, 9378–9383
56. Haddadi, M., Nongthomba, U., and Ramesh, S. R. (2016) Biochemical and behavioral evaluation of human MAPT mutations in transgenic *Drosophila melanogaster*. *Biochem. Genet.* **54**, 61–72
57. Wittmann, C. W., Wszolek, M. F., Shulman, J. M., Salvatore, P. M., Lewis, J., Hutton, M., and Feany, M. B. (2001) Tauopathy in *Drosophila*: Neurodegeneration without neurofibrillary tangles. *Science* **293**, 711–714
58. Augustinack, J. C., Schneider, A., Mandelkow, E.-M., and Hyman, B. T. (2002) Specific tau phosphorylation sites correlate with severity of neuronal cytopathology in Alzheimer's disease. *Acta Neuropathol.* **103**, 26–35
59. Yoshida, H., and Goedert, M. (2006) Sequential phosphorylation of tau protein by cAMP-dependent protein kinase and SAPK4/p38delta or JNK2 in the presence of heparin generates the AT100 epitope. *J. Neurochem.* **99**, 154–164
60. Hu, Y., Comjean, A., Rodiger, J., Liu, Y., Gao, Y., Chung, V., Zirin, J., Perrimon, N., and Mohr, S. E. (2021) FlyRNAi.org—the database of the *Drosophila* RNAi screening center and transgenic RNAi project: 2021 update. *Nucleic Acids Res.* **49**, D908–D915
61. Dolan, P. J., and Johnson, G. V. (2010) The role of tau kinases in Alzheimer's disease. *Curr. Opin. Drug Discov. Devel.* **13**, 595–603
62. Koriath, C. A. M., Bocchetta, M., Brotherhood, E., Woollacott, I. O. C., Norsworthy, P., Simón-Sánchez, J., Blauwendraat, C., Dick, K. M., Gordon, E., Harding, S. R., Fox, N. C., Crutch, S., Warren, J. D., Revesz, T., Lashley, T., et al. (2016) The clinical, neuroanatomical, and neuropathologic phenotype of TBK1-associated frontotemporal dementia: A longitudinal case report. *Alzheimers Dement. (Amst)* **6**, 75–81
63. Awadalla, M. S., Fingert, J. H., Roos, B. E., Chen, S., Holmes, R., Graham, S. L., Chehade, M., Galanopoulos, A., Ridge, B., Souzeau, E., Zhou, T., Siggs, O. M., Hewitt, A. W., Mackey, D. A., Burdon, K. P., et al. (2015) Copy number variations of TBK1 in Australian patients with primary open-angle glaucoma. *Am. J. Ophthalmol.* **159**, 124–130.e121
64. Ritch, R., Darbro, B., Menon, G., Khanna, C. L., Solivan-Timpe, F., Roos, B. R., Sarfarzi, M., Kawase, K., Yamamoto, T., and Robin, A. L. (2014) TBK1 gene duplication and normal-tension glaucoma. *JAMA Ophthalmol.* **132**, 544–548
65. Park, S., Lee, J. H., Jeon, J. H., and Lee, M. J. (2018) Degradation or aggregation: The ramifications of post-translational modifications on tau. *BMB Rep.* **51**, 265
66. Meier, S., Bell, M., Lyons, D. N., Rodriguez-Rivera, J., Ingram, A., Fontaine, S. N., Mechas, E., Chen, J., Wolozin, B., LeVine, H., 3rd, Zhu, H., and Abisambra, J. F. (2016) Pathological tau promotes neuronal damage by impairing ribosomal function and decreasing protein synthesis. *J. Neurosci.* **36**, 1001–1007
67. Steinhilb, M. L., Dias-Santagata, D., Mulkearns, E. E., Shulman, J. M., Biernat, J., Mandelkow, E. M., and Feany, M. B. (2007) S/P and T/P phosphorylation is critical for tau neurotoxicity in *Drosophila*. *J. Neurosci. Res.* **85**, 1271–1278
68. Zhang, Y., Chen, K., Sloan, S. A., Bennett, M. L., Scholze, A. R., O'Keefe, S., Phatnani, H. P., Guarnieri, P., Caneda, C., and Ruderisch, N. (2014) An RNA-sequencing transcriptome and splicing database of glia, neurons, and vascular cells of the cerebral cortex. *J. Neurosci.* **34**, 11929–11947
69. Lauro, C., and Limatola, C. (2020) Metabolic reprogramming of microglia in the regulation of the innate inflammatory response. *Front. Immunol.* **11**, 493
70. Xu, D., Jin, T., Zhu, H., Chen, H., Ofengeim, D., Zou, C., Mifflin, L., Pan, L., Amin, P., Li, W., Shan, B., Naito, M. G., Meng, H., Li, Y., Pan, H., et al. (2018) TBK1 suppresses RIPK1-driven apoptosis and inflammation during development and in aging. *Cell* **174**, 1477–1491.e1419
71. Brenner, D., Sieverding, K., Bruno, C., Lüningschrör, P., Buck, E., Mungwa, S., Fischer, L., Brockmann, S. J., Ulmer, J., and Bliederhäuser, C. (2019) Heterozygous *Tbk1* loss has opposing effects in early and late stages of ALS in mice. *J. Exp. Med.* **216**, 267–278
72. Gerbino, V., Kaunga, E., Ye, J., Canzio, D., O'Keefe, S., Rudnick, N. D., Guarnieri, P., Lutz, C. M., and Maniatis, T. (2020) The loss of TBK1 kinase activity in motor neurons or in all cell types differentially impacts ALS disease progression in SOD1 mice. *Neuron* **106**, 789–805.e5
73. Chuna, J., Kwon, T., Lee, E. J., Kim, C. H., Han, Y. S., Hong, S.-K., Hyun, S., and Kang, S. S. (2004) 14-3-3 Protein mediates phosphorylation of microtubule-associated protein tau by serum- and glucocorticoid-induced protein kinase 1. *Mol. Cells* **18**, 360–368
74. Hashiguchi, M., Sobue, K., and Paudel, H. K. (2000) 14-3-3 $\zeta$  is an effector of tau protein phosphorylation. *J. Biol. Chem.* **275**, 25247–25254
75. Bai, L. Y., Chiu, C. F., Kapuriya, N. P., Shieh, T. M., Tsai, Y. C., Wu, C. Y., Sargeant, A. M., and Weng, J. R. (2015) BX795, a TBK1 inhibitor, exhibits antitumor activity in human oral squamous cell carcinoma through apoptosis induction and mitotic phase arrest. *Eur. J. Pharmacol.* **769**, 287–296
76. Clark, K., Plater, L., Pegg, M., and Cohen, P. (2009) Use of the pharmacological inhibitor BX795 to study the regulation and physiological roles of TBK1 and I $\kappa$ B kinase epsilon: A distinct upstream kinase mediates Ser-172 phosphorylation and activation. *J. Biol. Chem.* **284**, 14136–14146
77. Hasan, M., and Yan, N. (2016) Therapeutic potential of targeting TBK1 in autoimmune diseases and interferonopathies. *Pharmacol. Res.* **111**, 336–342
78. Bain, J., Plater, L., Elliott, M., Shpiro, N., Hastie, C. J., McLauchlan, H., Klevernic, I., Arthur, J. S., Alessi, D. R., and Cohen, P. (2007) The selectivity of protein kinase inhibitors: A further update. *Biochem. J.* **408**, 297–315
79. Dammer, E. B., Lee, A. K., Duong, D. M., Gearing, M., Lah, J. J., Levey, A. I., and Seyfried, N. T. (2015) Quantitative phosphoproteomics of Alzheimer's disease reveals cross-talk between kinases and small heat shock proteins. *Proteomics* **15**, 508–519
80. Ping, L., Kunding, S. R., Duong, D. M., Yin, L., Gearing, M., Lah, J. J., Levey, A. I., and Seyfried, N. T. (2020) Global quantitative analysis of the human brain proteome and phosphoproteome in Alzheimer's disease. *Sci. Data* **7**, 315
81. Abreha, M. H., Dammer, E. B., Ping, L., Zhang, T., Duong, D. M., Gearing, M., Lah, J. J., Levey, A. I., and Seyfried, N. T. (2018) Quantitative analysis of the brain ubiquitylome in Alzheimer's disease. *Proteomics* **18**, 1800108
82. Seyfried, N. T., Dammer, E. B., Swarup, V., Nandakumar, D., Duong, D. M., Yin, L., Deng, Q., Nguyen, T., Hales, C. M., Wingo, T., Glass, J., Gearing, M., Thambisetty, M., Troncoso, J. C., Geschwind, D. H., et al. (2017) A multi-network approach identifies protein-specific Co-expression in asymptomatic and symptomatic Alzheimer's disease. *Cell Syst.* **4**, 60–72.e64
83. Chouhan, A. K., Guo, C., Hsieh, Y.-C., Ye, H., Senturk, M., Zuo, Z., Li, Y., Chatterjee, S., Botas, J., and Jackson, G. R. (2016) Uncoupling neuronal death and dysfunction in *Drosophila* models of neurodegenerative disease. *Acta Neuropathol. Commun.* **4**, 62